ACS APPLIED MATERIALS & INTERFACES

Research Article

www.acsami.org

Flexible and Microporous Chitosan Hydrogel/Nano ZnO Composite Bandages for Wound Dressing: In Vitro and In Vivo Evaluation

P. T. Sudheesh Kumar,[†] Vinoth-Kumar Lakshmanan,[†] T.V. Anilkumar,[‡] C. Ramya,[†] P. Reshmi,[§] A.G. Unnikrishnan,[∇] Shantikumar V. Nair,[†] and R. Jayakumar[†,*]

[†]Amrita Centre for Nanosciences and Molecular Medicine, Amrita Institute of Medical Sciences and Research Centre, Amrita Vishwa Vidyapeetham University, Kochi-682 041, India

[‡]Laboratory for Experimental Pathology, Biomedical Technology Wing, Sree Chitra Tirunal Institute for Medical Sciences and Technology, Thiruvananthapuram-695012, Kerala, India

[§]Amrita Central Lab Animal Facility, Amrita Institute of Medical Sciences and Research Centre, Amrita Vishwa Vidyapeetham University, Kochi-682 041, India

[∇]Department of Endocrinology, Amrita Institute of Medical Sciences and Research Centre, Amrita Vishwa Vidyapeetham University, Kochi-682 041, India

ABSTRACT: Current wound dressings have disadvantages such as less flexibility, poor mechanical strength, lack of porosity, and a tendency for dressings to adhere onto the wound surface; in addition, a majority of the dressings did not possess antibacterial activity. Hydrogel-based wound dressings would be helpful to provide a cooling sensation and a moisture environment, as well as act as a barrier to microbes. To overcome these hassles, we have developed flexible and microporous chitosan hydrogel/nano zinc oxide composite bandages (CZBs) via the incorporation of zinc oxide nanoparticles (nZnO) into chitosan hydrogel. The prepared nanocomposite bandages were characterized using Fourier transform infrared spectroscopy (FT-IR), X-ray diffractometry (XRD), and scanning electron microscopy (SEM). In addition, swelling, degradation, blood clotting, antibacterial, cytocompatibility, cell attachment on the material, and cell infiltration into the composite bandages were evaluated. The nanocomposite bandage showed enhanced swelling, blood clotting, and antibacterial activity. Cytocompatibility of the composite bandage has been analyzed in normal human dermal fibroblast cells. Cell attachment and infiltration studies showed that the cells were found attached to the nanocomposite bandages and penetrated into the interior. Furthermore, the in vivo evaluations in Sprague−Dawley rats revealed that these nanocomposite bandages enhanced the wound healing and helped for faster re-epithelialization and collagen deposition. The obtained data strongly encourage the use of these composite bandages for burn wounds, chronic wounds, and diabetic foot ulcers.

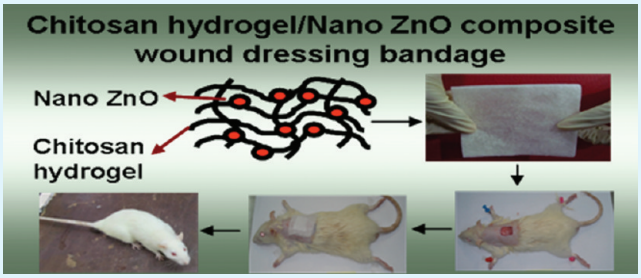

KEYWORDS: *wound healing, chitosan hydrogel, ZnO nanoparticle, hemostatic, antibacterial activity, in vivo test*

1. INTRODUCTION

Wound infection is the major difficulty in the field of wound care management, because such infections can cause exudate formation, delay the wound healing, facilitate improper collagen deposition, etc.[1−3] Microbes are the major reason for infection and the prevalence of the same is high in and around us. The major infection causing bacteria were *Staphylococcus aureus* (*S. aureus*) and *Escherichia coli* (*E. coli*).[4,5] Once entered into the body, these microbes grow immediately and start to form colonies. The microbes can easily entered the body through the wounds and can reach into deeper portions of the tissue and, furthermore, can lead to internal infection.[4] The remedy for the above-mentioned harms would be the use of wound dressing with antibacterial activity.[6]

At times, even a wound dressing itself can cause infection, because of the wound dressing-exudate interface, nonsterility of the wound dressing, etc.[7] The remedy for these problems would be the use of hydrogel-based wound dressings that possess all the necessary properties, such as maintaining a moist environment at the wound interface, providing a cooling sensation, allowing gaseous exchange, maintaining barrier to microorganisms, and allowing wound exudate absorption, biodegradability, hemostatic potential, and biocompatibility.[1,8] Various types of wound dressing materials are available commercially, i.e., those made of synthetic polymers (such as poly(vinyl alcohol)) or using natural polymers (such as alginate, chitin, chitosan. etc.).[9−17] Previous studies have been reported where chitosan films and membranes were used to treat patients with deep burns, orthopedic injuries, etc.[9,17−26] The reasons for choosing chitosan were the ease of availability,

Received: February 20, 2012
Accepted: April 11, 2012
Published: April 11, 2012

hemostatic potential, and biodegradability, and the biodegradation product was *N*-acetyl glucosamine, which was already present in the human body and will enhance the re-epithelization.[6,27−30] The so-called membranes and films have poor mechanical strength, less flexibility, poor wound healing potential, and no antibacterial activity.[17,19]

At neutral pH, chitosan does not show any antibacterial activity; in order to impart that activity, it is necessary to incorporate some antibacterial agents into it.[7] It is well-known that zinc oxide nanoparticles (nZnO) possesses antibacterial activity and it is currently used in many cosmetic materials.[31−36] In order to impart antibacterial activity, nZnO has been added to these wound dressing materials. Previous studies had shown that, on a size scale of <100 nm and at the appropriate concentration, nZnO possesses potent antibacterial activity but has no adverse effect on normal cells.[37,38] Furthermore, the Zn ions released from ZnO can enhance keratinocyte migration toward the wound site and promote healing.[12] We prepared microporous and flexible composite bandages using chitosan hydrogel and nZnO, and the efficacy was evaluated in vitro and in vivo.

2. EXPERIMENTAL SECTION

Materials. Chitosan (molecular weight = 100−150 kDa, degree of deacetylation = 85%) was purchased from Koyo Chemical Co., Ltd., Japan. Acetic acid, sodium hydroxide, and zinc acetate dihydrate were purchased from Qualigens, India. Hen lysozyme was purchased from Fluka. DAPI (4′,6-diamidino-2-phenylindole), Alamar Blue, Trypsin-EDTA, and Fetal Bovine Serum (FBS) were obtained from Gibco, Invitrogen Corporation. Minimum essential medium (MEM) was purchased from Sigma−Aldrich Company. The normal human dermal fibroblast cell (HDF) was purchased from Promocell, Germany. Luria−Bertani broth and agar−agar were purchased from Himedia, India. *E. coli* (ATCC 25922) and *S. aureus* (ATCC 25923) strains were obtained from the Microbiology Laboratory of Amrita Institute of Medical Sciences, Kochi, India. The chemicals were used without further purification.

Preparation of ZnO Nanoparticles. Zinc oxide nanoparticles (nZnO) were prepared as follows: 0.1 M sodium hydroxide solution was added dropwise to 0.1 M zinc acetate dihydrate solution with continuous stirring. The solvent used for the preparation was methanol. The precipitated zinc oxide was centrifuged and washed several times with distilled water to remove the byproduct and dried at 80 °C.[37]

Preparation of Chitosan Hydrogel/nZnO Composite Bandages. Chitosan solution was prepared by dissolving 2 g of chitosan in 1% acetic acid solution under room temperature. The solution was then filtered to remove undissolved particles. Chitosan hydrogel was prepared by raising the pH of chitosan solution to neutral pH by the addition of 1% NaOH solution, followed by centrifugation of the hydrogel to remove unbound water. The prepared nZnO were then suspended in water followed by probe sonication (Sonics, Germany) for 10 min. The ZnO nanosuspension was added dropwise to the chitosan hydrogel and the entire mixture kept under vigorous stirring for 1 h. The homogenized chitosan hydrogel/nZnO mixture was poured on to Teflon mold and kept at −20 °C overnight. The frozen samples were lyophilized for 24 h (Martin Christ, Germany) to obtain porous chitosan hydrogel/nano ZnO bandages (CZBs).

Characterization. The prepared nZnO and CZBs were characterized using X-ray diffraction (XRD) (PANalytical X'Pert PRO, Cu Kα radiation, operating at a voltage of 40 kV), Fourier transform infrared spectroscopy (FTIR) (Perkin−Elmer Co., Model SPECTRUM RX1, FT-IR). The morphology and size of the nZnO were characterized using dynamic light scattering (DLS) measurements (DLS-ZP/Particle Sizer Nicomp 380 ZLS, particle sizing system) and atomic force microscopy (AFM) (JEOL JSPM-5200). The structural morphology of CZBs was characterized by scanning electron microscopy (SEM) (JEOL, JSM-6490LA, Japan).

Porosity of Chitosan Hydrogel/Nano Zinc Oxide Composite Bandages. The porosity of the prepared CZBs was determined using the reported method.[12] Briefly, the CZBs were immersed in absolute ethanol until it was saturated. The CZBs were weighed before and after the immersion in alcohol. The porosity was calculated using the formula

$$P = \frac{W_2 - W_1}{\rho V_1}$$

In the equation, W_1 and W_2 indicate the weight of CZBs before and after immersion in alcohol, respectively. V_1 is the volume before immersion in alcohol; ρ is a constant (the density of alcohol). All samples were triplicated in the experiment.

Swelling Ratio of Chitosan Hydrogel/Nano Zinc Oxide Composite Bandage. CZBs were cut into small pieces that had equal weights and were immersed in phosphate buffered saline (PBS) (pH 7.4, 37 °C). The bandages were taken out at predetermined time intervals and water that adhered on the surface was removed by gently blotting with filter paper and immediately weighed (W_d). In this expression, DS is the degree of swelling; W_w and W_d represent the wet and dry weight of the bandages, respectively.[12]

$$\mathrm{DS} = \frac{W_w - W_d}{W_d} \times 100$$

In Vitro Biodegradation of Chitosan Hydrogel/Nano Zinc Oxide Composite Bandage. The degradation of the bandages was studied in a PBS (pH 7.4) medium containing lysozyme at 37 °C. Bandages were equally weighed and immersed in lysozyme (10 000 U/mL) containing the medium and incubated at 37 °C for 21 days. CZBs were removed after 7, 14, and 21 days from the medium containing lysozyme and washed with deionized water to remove ions adsorbed on surface and freeze-dried. The dry weight was noted as W_t and initial weight as W_i. The degradation of bandage was calculated using the formula[3]

$$\text{degradation (\%)} = \frac{W_i - W_t}{W_i} \times 100$$

Mechanical Properties Evaluation. Tensile strength and elongation at break of the CZBs were measured. The experimental procedure was as follows: the bandage specimens were prepared with dimensions of 10 cm × 2 cm × 0.4 cm. Both ends of tensile specimens were clipped with a special gripper. The tensile strength and percentage elongation at break of the bandages were measured by a universal testing machine (Instron, Model 3365) with a load cell of 5 kN and the crosshead speed was 25 mm min^{-1} at room temperature. The average value out of six measurements was reported for each sample.

Whole-Blood Clotting and Platelet Activation Evaluation of Chitosan Hydrogel/Nano Zinc Oxide Composite Bandage. The blood clotting studies were done based on reported literature.[39] The blood-clotting ability of CZBs was analyzed and compared with commercially available dressing (Kaltostat, Convatec). Blood was drawn from human ulnar vein using BD Discardit II sterile syringe and mixed with anticoagulant agent acid citrate dextrose at a ratio of 85%:15%. Triplicate samples were used for this study and blood without sample was used as negative control. Blood was added to each bandage and placed in a 25-mL plastic Petri dish, which was followed by the addition of 10 μL of 0.2 M $CaCl_2$ solutions to initiate blood clotting. These CZBs then were incubated at 37 °C for 10 min. Fifteen milliliters (15 mL) of distilled water was then added dropwise without disturbing the clot. Subsequently, 10 mL of solution was taken from the dishes and was centrifuged at 1000 rpm for 1 min. The supernatant was collected for each sample and kept at 37 °C for 1 h. Two hundred microliters (200 μL) of this solution was transferred to a 96-well plate. The optical density was measured at 540 nm using a plate reader (BioTek PowerWave XS).

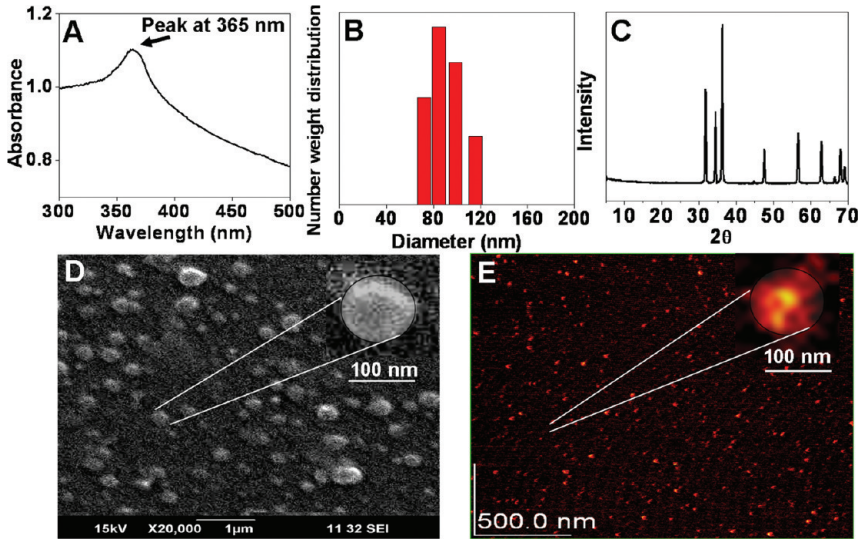

Figure 1. Characterization of nZnO: (A) UV–vis spectrum, (B) DLS spectrum, (C) XRD spectrum, (D) SEM image, and (E) AFM image.

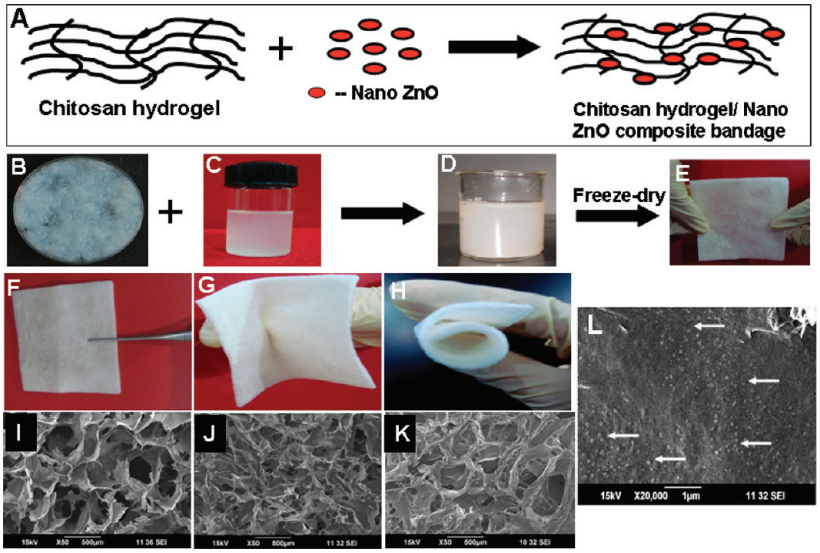

Figure 2. (A) Schematic representation of the chitosan hydrogel/nZnO composite bandage. (B, C, D) Photographs of the chitosan hydrogel, nZnO suspension, and chitosan hydrogel/nZnO mixture, respectively. (E, F, G, H) Photographs of chitosan hydrogel/nZnO composite bandage. (I, J, K) SEM images of chitosan control, chitosan + 0.01% nZnO, and chitosan + 0.005% nZnO composite bandages, respectively. (L) SEM image of the chitosan + 0.01% nZnO composite bandage; white arrows indicate the nZnO particles.

Platelet activation study was conducted as follows.[39] Platelet-rich plasma (PRP) was isolated from the blood by centrifugation of blood at 2500 rpm for 5 min. One hundred microliters (100 μL) of PRP was poured onto the bandage piece (10 mg) and incubated at 37 °C for 20 min. The bandages were then washed three times with PBS solution and fixed using 0.1% glutaraldehyde solution. The bandages were dried and SEM images were taken.

In Vitro Antibacterial Studies. *E. coli* (gram negative) and *S. aureus* (gram positive) were used to evaluate the antibacterial activity of the prepared CZBs. Luria–Bertani broth (LB broth) and Luria–Bertani agar (LB agar) were used as culturing nutrient sources. *E. coli* and *S. aureus* were inoculated in sterilized LB broth and incubated overnight at 37 °C in a shaking incubator. The concentration of bacteria was 10^6 colony-forming units per milliliter (CFU/mL). CZBs were added to the LB broth and incubated at 37 °C for 24 h. After the incubation period, the quantification of viable bacteria was done by serial dilution of the bacteria culture in normal saline followed by plating on LB agar plate. The numbers of colonies were counted to determine the antibacterial activity.[37]

Cell Viability Study. Cell viability of the prepared CZBs was evaluated by Alamar Blue assay.[12] The cell viability of CZBs with different concentration of nZnO was evaluated on nHDF cells. Bandages were sterilized by ethylene oxide gas. nHDF cells were cultured in fibroblast growth medium provided by promocell, Germany. Sterile bandage pieces were placed in 12 well plates containing 5×10^4 cells. The cells with the bandage materials were then incubated up to 72 h and Alamar Blue assay (Invitrogen, USA) was performed. The optical density measured at 570 nm, with 620 nm set as the reference wavelength, using a microplate spectrophotometer (Biotek PowerWave XS, USA).

Cell Attachment and Infiltration Evaluation. The CZBs bandages were seeded with nHDF cells in a 24-well plate at a concentration of 1×10^5cells/well. After 24 h of incubation, the bandages were washed with PBS and fixed with 2.5% glutaraldehyde for 1 h. The samples were thoroughly washed with PBS and sequentially dehydrated in a graded-ethanol series, air-dried, gold sputtered in vacuum and examined via SEM.

DAPI (4′,6-diamidino-2-phenylindole) is a fluorescent stain commonly used as a nuclear stain. For DAPI staining, the cell-seeded

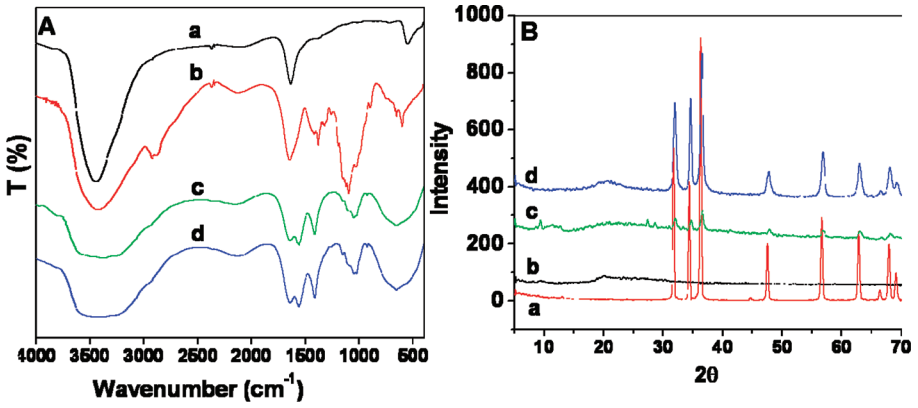

Figure 3. FT-IR and XRD characterizations of CZBs. (A) FT-IR spectra of nZnO (spectrum a), chitosan control (spectrum b), chitosan + 0.005% nZnO (spectrum c), and chitosan + 0.01% nZnO (spectrum d). (B) XRD spectra of nZnO (spectrum a), chitosan control (spectrum b), chitosan + 0.005% nZnO (spectrum c), and chitosan + 0.01% nZnO (spectrum d).

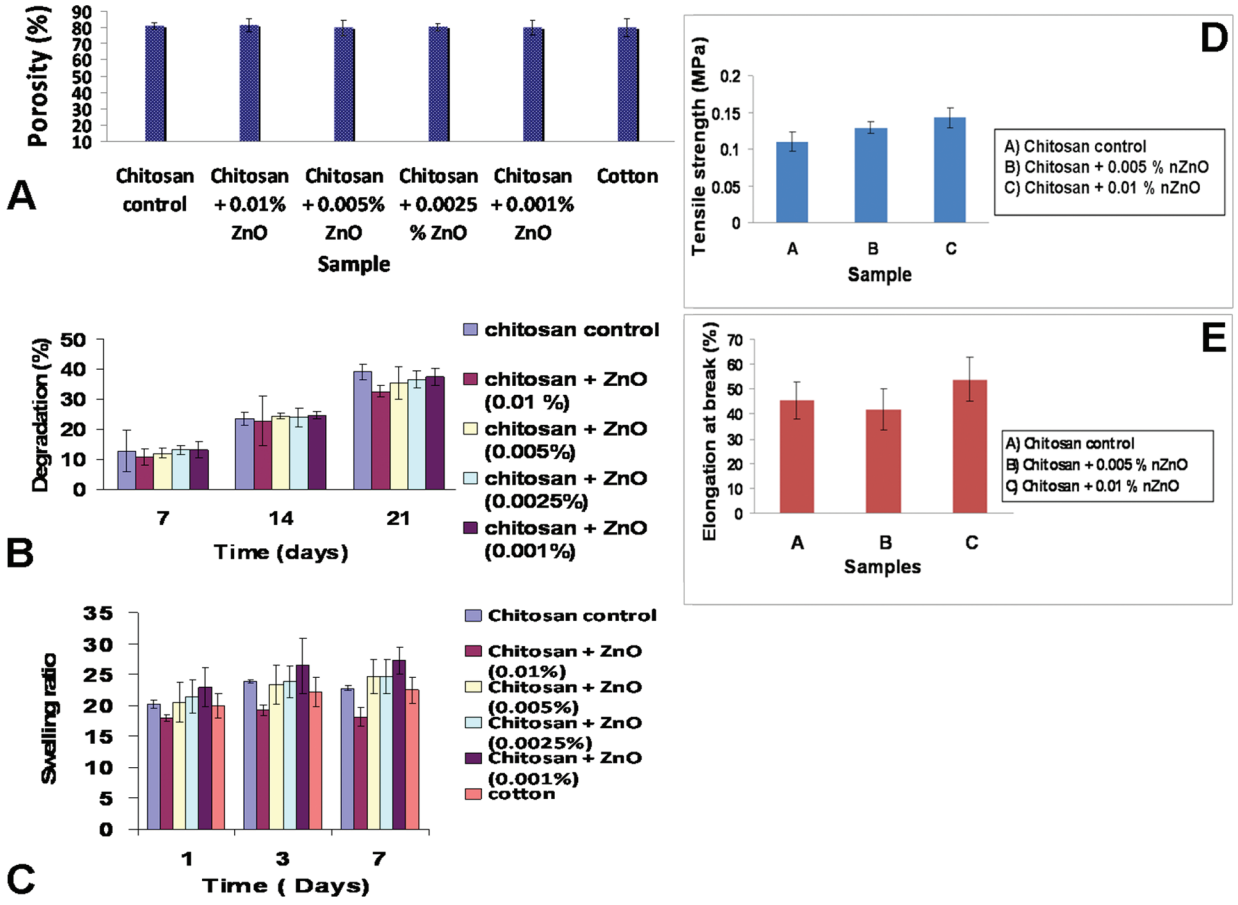

Figure 4. (A) Porosity evaluation, (B) swelling ratio, (C) biodegradation, (D) tensile strength, and (E) elongation at break of composite bandages.

bandages were fixed with 4% paraformaldehyde for 20 min, permeabilized with 0.5% Triton X-100 (in PBS) for 5 min. The bandages were then treated with 1% FBS followed by washing with PBS and stained with 50 μL of DAPI (1:30 dilution with PBS). The bandages incubated in darkness for 5 min and viewed under fluorescent microscope (Olympus-BX-51) after washing with PBS. For cell infiltration evaluation, the bandages were incubated with nHDF cells for 24 h. The bandages were stained with TRITC (tetramethyl rhodamine iso-thiocyanate) conjugated Phalloidin dye and images were taken using a laser confocal microscope (Leica, Model SP 5 II).

In Vivo Evaluation. In vivo animal study was approved by the Institutional Animal Ethical Committee (IAEC), at Amrita Institute of Medical Sciences and Research Center, Cochin, India. Sprague–Dawley (SD) rats, weighing 200–250 g and 4–6 weeks of age, were used in this study. The rats were divided into five groups and each group contains three rats (n = 3); rats were allowed to take normal rat feed and water without restriction. On the day of wounding, the rats were anaesthetized by intramuscular injection of 35.0 mg/kg ketamine and 5.0 mg/kg xylazine. The dorsal area of the rats depilated and the operative area of skin cleaned with alcohol. A partial thickness skin wound of 1.5 cm square was prepared by excising the dorsum of the rat using surgical scissors and forceps. The prepared wounds were then covered with the CZBs, chitosan control, and Kaltostat. Rats with bare wound were kept as negative control. After applying the dressing

dx.doi.org/10.1021/am300292v | ACS Appl. Mater. Interfaces 2012, 4, 2618–2629

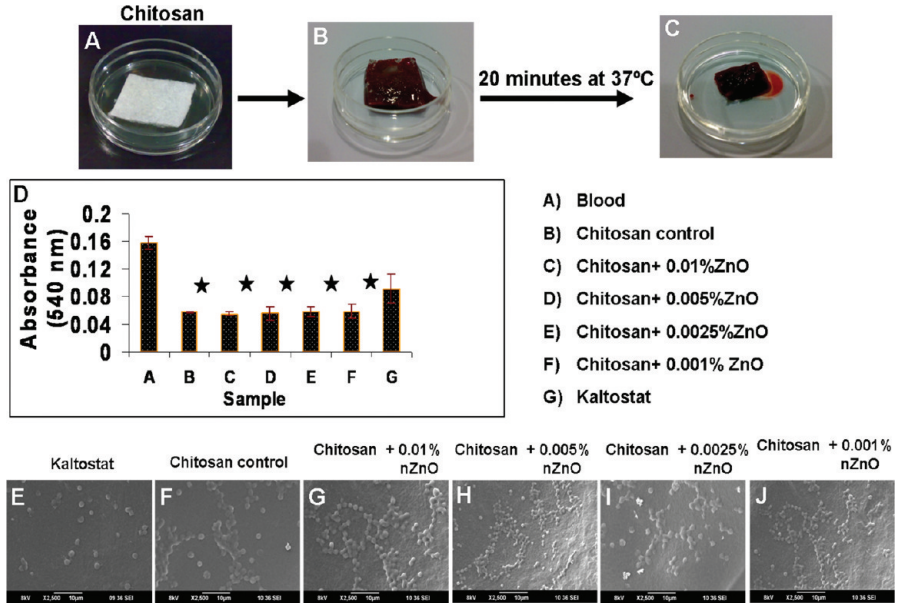

Figure 5. (A, B, C) Photographs of the chitosan bandage, blood on the chitosan bandage, clotted blood on the CZB, respectively. (D) Whole-blood clotting evaluation of bandages (star symbols (★) represent the $p < 0.05$ level, indicating that the means are significantly different, compared to the control (E, F, G, H, I, and J) SEM images of platelet activation of bandages.

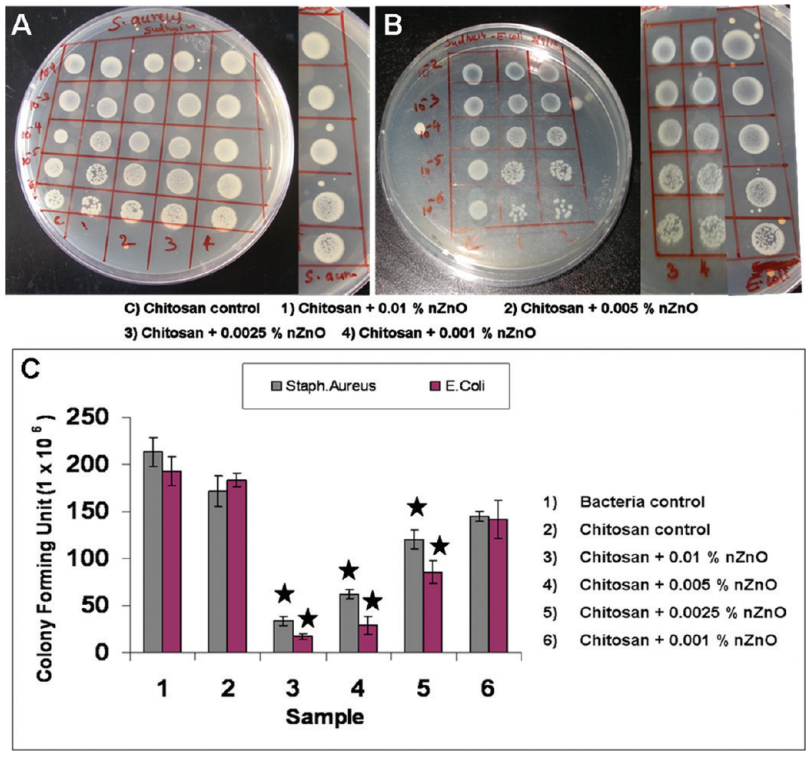

Figure 6. Photographs showing the antibacterial activity of composite bandages against (A) *S. aureus* and (B) *E. coli*. (C) Quantification of the antibacterial activity. (Star symbols (★) represents the $p < 0.05$ level, indicating that the means are significantly different, compared with the control.)

materials, the rats were housed individually in cages under normal room temperature.

The dressing materials were changed at Weeks 1, 2, and 3. During the changing of dressings, photographs were taken and the wound area was measured using a transparent polyethylene sheet. The sheet was kept on top of the wound and area was marked using a marker pen. The marked area was then transferred to graph sheet for getting the exact value. After Week 4, the skin wound tissue of the rat was excised, fixed with 10% formalin, and stained with a hematoxylin−eosin (H&E) reagent for histological observations. The deposition of collagen was determined using Picro-Sirius Red staining, and the collagen content was quantified by histomorphometry.

Swabs were collected from the rat wounds after Weeks 1 and 2, using sterile swabs and cultured overnight in Luria−Bertani broth (LB broth) at 37 °C. The bacteria were then serially diluted in normal saline and plated in LB agar plate. The plates were then kept at 37 °C overnight and the colonies were counted for quantitative determi-

dx.doi.org/10.1021/am300292v | ACS Appl. Mater. Interfaces 2012, 4, 2618−2629

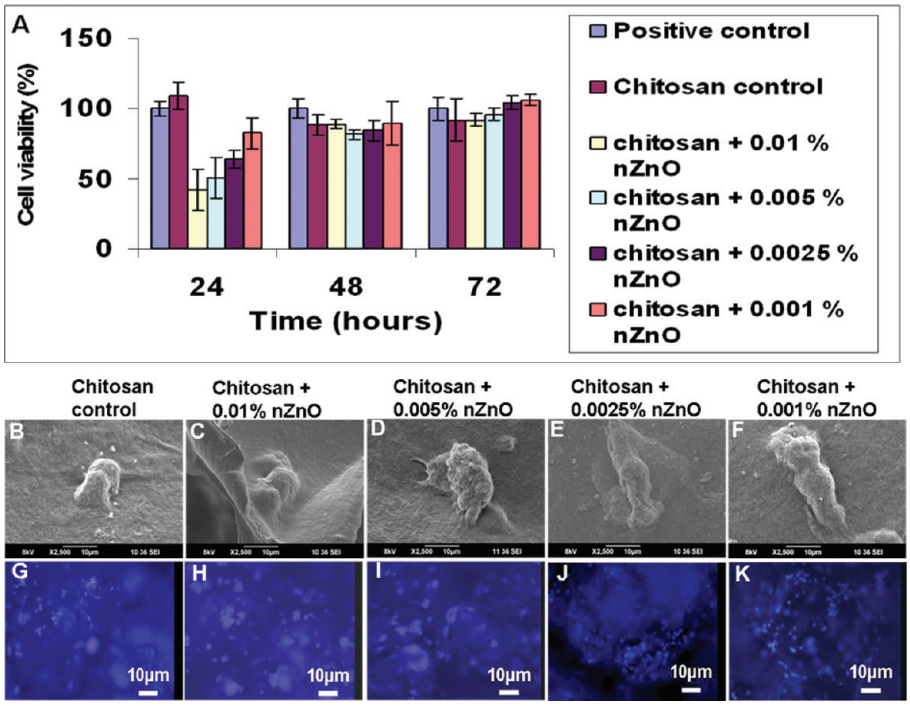

Figure 7. (A) Cell viability study using nHDF cells. (B, C, D, E, F) SEM images of cell attachment on bandages. (G, H, I, J, K) DAPI staining of nHDF cells attached on bandages.

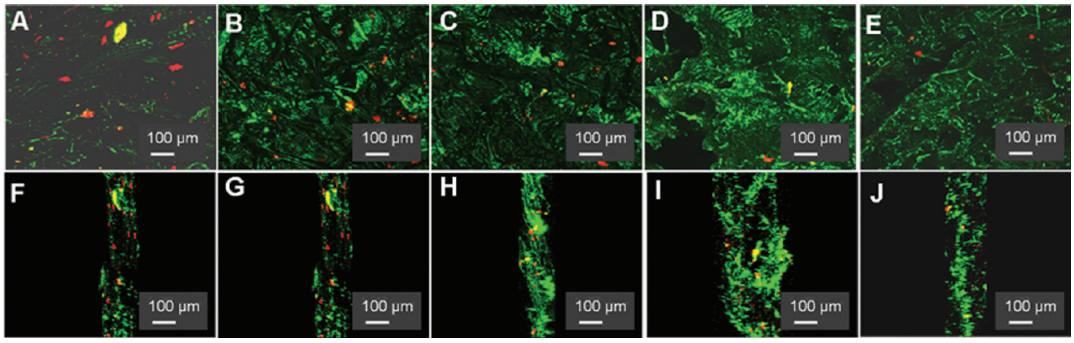

Figure 8. (A, F) Laser confocal images of the surface and lateral view of chitosan bandage with cells, respectively. (B, G) Confocal images of the surface and lateral view of chitosan + 0.001% nZnO bandage, respectively. (C, H) Confocal images of the surface and lateral view of chitosan + 0.0025% nZnO bandage, respectively. (D, I) Confocal images of the surface and lateral view of chitosan + 0.005% nZnO bandage, respectively. (E, G) Confocal images of the surface and lateral view of chitosan + 0.01% nZnO bandage, respectively.

nation. The isolated bacterial strains were streaked in LB agar plates and identification of the strains was done by biochemical assays.

Statistics analysis. The values were expressed in a format of mean ± standard deviation (SD). The results obtained were analyzed statistically. A Student's *t*-test was conducted to determine the significance. A probability level of $p < 0.05$ was considered to be statistically significant.

3. RESULTS AND DISCUSSION

Characterization. Figure 1 shows the characterization data of nZnO. The particles were suspended in water and sonicated for 10 min at room temperature prior to the analysis. The ultraviolet−visible light (UV−vis) spectrum showed an absorbance at 360 nm, which corresponds to the nZnO (Figure 1A). The broadness of peak indicates the polydispersed nature of nZnO. DLS analysis was conducted to measure the size and distribution of nZnO. The size of the particles was in the range of 70−120 nm (Figure 1B). XRD spectrum (Figure 1C) showed the characteristic peaks of zinc oxide (JCPDS File Card No. 89-1397). The size of the prepared nZnO was also confirmed by AFM and SEM analysis (see Figures 1D and 1E).

Figure 2A represents the schematic representation of the synthesis of CZBs. Figures 2B, 2C, and 2D are photographs of the chitosan hydrogel, nZnO suspension, and chitosan hydrogel/nZnO mixture, respectively. Figures 2F, 2G, and 2H represent photographs of CZBs. Figure 2 clearly shows that these CZBs were flexible. Figures 2I, 2J, and 2K show SEM images of the chitosan bandage control and CZBs with different concentrations of nZnO. All these bandages showed well-interconnected pores and the pore size was in the range of 200−400 μm. The addition of nZnO caused a slight change in the morphology fo CZBs. This was due to the interaction of nZnO and chitosan. Figure 2L (white arrows) shows the nZnO distributed on the surface of CZBs.

The FT-IR data of CZBs revealed that all of the characteristic peaks of chitosan (1070, 1105, 1450, and 1630 cm^{-1}) as well as nZnO (510 and 1550 cm^{-1}) were present in the spectra.[7,19]

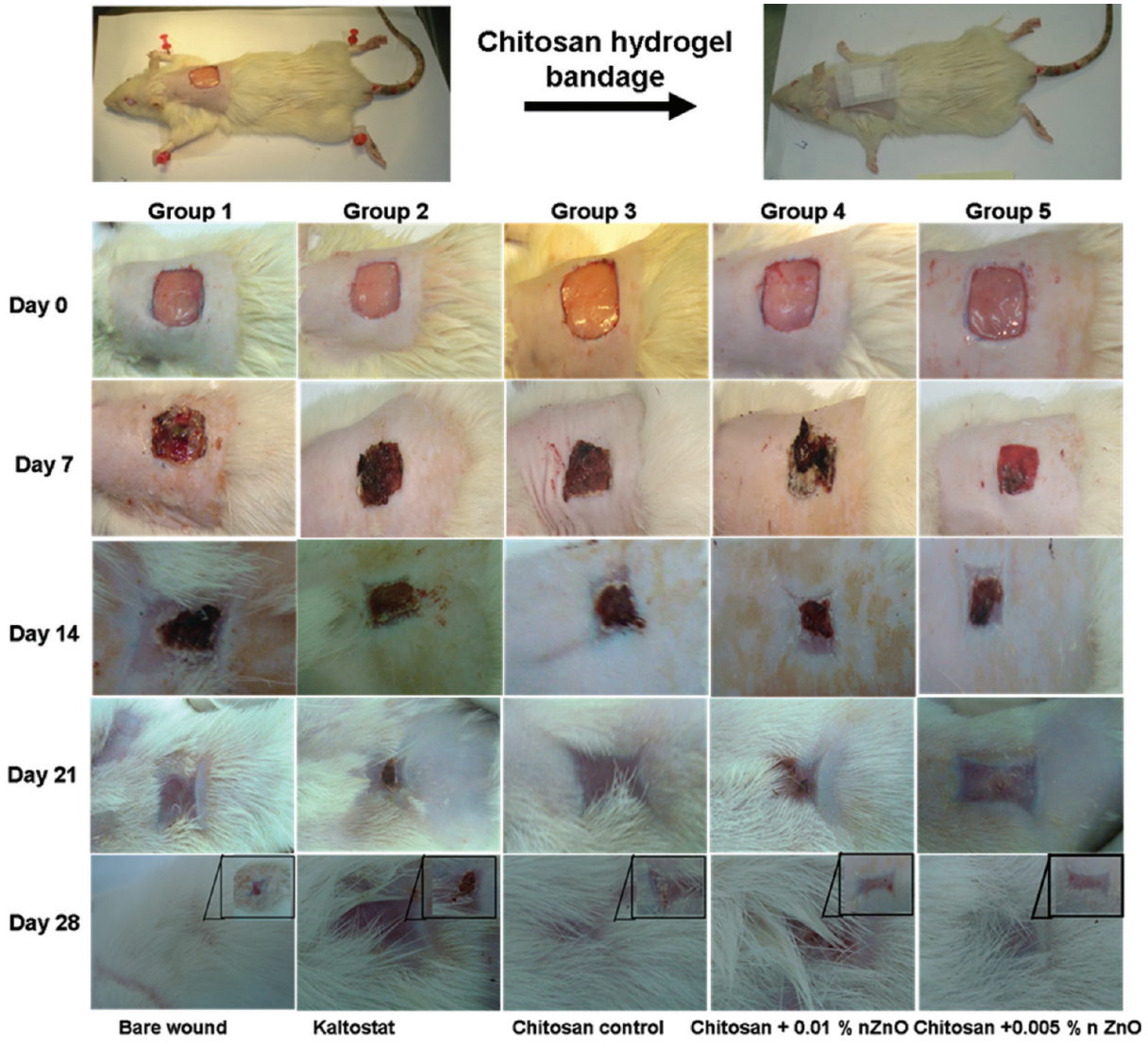

Figure 9. Photographs of an in vivo wound healing study. Note the extent of wound closure in the wounds treated with chitosan control and CZBs.

The broadening of peaks in the CZB spectra at 3450 cm^{1} attributed to the intermolecular hydrogen bonding between the nZnO and chitosan (Figure 3A).

XRD spectra showed that characteristic peaks of chitosan control were present in the corresponding spectra. The characteristic peaks of nZnO peaks at 31.6°, 34.3°, 36.2°, 56.5°, 62.8°, and 67.8° were present in the spectra, along with peaks of chitosan control.[19] At lower concentration of nZnO, CZBs showed reduced intensity for the ZnO characteristic peaks (see Figure 3B).

Porosity and Swelling Ratio of Chitosan Hydrogel/Nano Zinc Oxide Composite Bandage. Porosity of CZBs was evaluated using an alcohol displacement method.[12] It was found that the porosity of the control and that of the composite bandages were the same, even after the incorporation of nZnO. All bandages showed porosity in the range of 75%−85% (see Figure 4A). The highly porous nature of the bandages would be helpful to absorb large volume of wound exudate from the wound surface. Furthermore, the porous nature of bandages enhances the distribution of nutrients and medium for the cells that get attached on it. Swelling ratio analysis revealed that at day 1, all bandages showed swelling ratios in the range of 17−25 (see Figure 4B). The swelling ratio slightly increased at day 2. There was not much difference between day 2 and day 3. The remarkable point was that, at day 1, the bandages were saturated with the liquid in which it was immersed. The swelling capacity of the bandage did not change, even after the incorporation of nZnO.

In Vitro Biodegradation of Chitosan Hydrogel/Nano Zinc Oxide Composite Bandage. Biodegradation data (Figure 4C) revealed the controlled biodegradation nature of CZBs. All the bandages including the control showed 5%−15% degradation after one week. The bandages showed 20%−25% degradation after two weeks and 25%−35% after three weeks. The reported degradation mechanism was the cleavage of glycosidic linkage between the monomers by lysozyme.[2,6,40] The obtained results revealed that the incorporation of nZnO did not alter the degradation nature of bandages. This was due to the fact that the nZnO concentration was low. It has been reported that the degradation of products of chitosan were D-glucosamine and glycosaminoglycan, which were already present in our body for the wound healing and were nontoxic to the cells.[2,8,9]

Evaluation of Mechanical Properties. The tensile strength of the chitosan control and CZBs was measured, and chitosan control showed a tensile strength of 0.1 MPa,

dx.doi.org/10.1021/am300292v | ACS Appl. Mater. Interfaces 2012, 4, 2618−2629

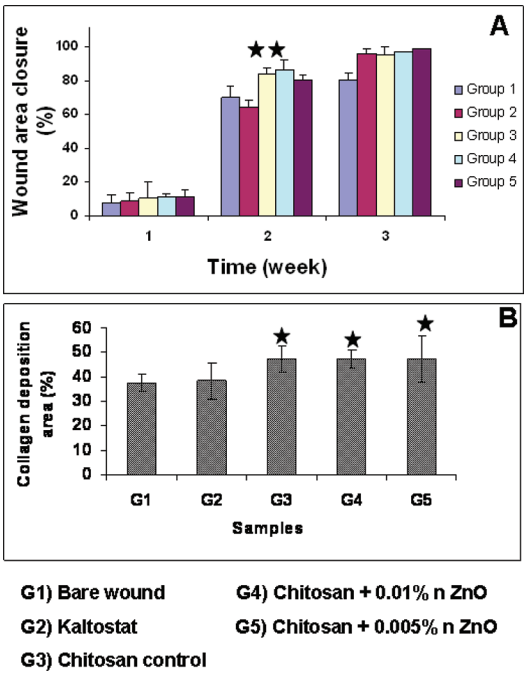

Figure 10. (A) Evaluation of the wound area closure and (B) study of the collagen deposition area. (In both graphs, the start symbols (★) represent the $p < 0.05$ level, indicating that the means are significantly different, compared with the control.)

which was adequate for a wound dressing material (Figure 4D). The incorporation of nZnO slightly enhanced the tensile strength up to 0.15 MPa, which was due to the interaction between nZnO and chitosan. The obtained results showed that the CZBs had sufficient strength to bare the force applied on them. Elongation at break values indicates the flexibility of the material. Control and CZBs showed elongation in the range of 40%−60% at break points (Figure 4E). The obtained data were adequate to show the flexible nature of the CZBs. The flexible nature would be supportive for the application of these CZBs over any type of wound surface.

Evaluation of Whole-Blood Clotting and Platelet Activation. Whole-blood clotting study was conducted to assess the hemostatic potential of CZBs. Figures 5A, 5B, and 5C show representative photographs of the blood clotting caused by the CZBs. Chitosan control and CZBs showed enhanced blood clotting ability in comparison with Kaltostat and blood alone (Figure 5D). This was due to the interaction between cationic chitosan and negatively charged blood cells.[26] This was further confirmed by the platelet activation analysis by SEM. Kaltostat did not activate the platelets while chitosan control and CZBs promoted platelet activation. The SEM images show that the activated platelets has spread all over the bandage surface (Figures 5E−J).

In Vitro Antibacterial Studies. We tested the antibacterial activity of CZBs against *S. aureus* (Figure 6A) and *E. coli* (Figure 6B). In the figures left to right shows the various sample and top to bottom indicates serial dilution of bacteria. Chitosan control did not show toxicity toward both strains. The reason was attributed to the pH of the chitosan control, which was neutral, and it has been reported earlier that at neutral pH chitosan does not show antibacterial activity. Our data revealed that CZB having higher concentration of nZnO showed more activity compared to the lower-concentration nZnO-containing CZBs (Figure 6C). The antibacterial activity of CZBs was due to the presence of nZnO. According to the reported literature, the antibacterial activity was due to the ROS (reactive oxygen species) production by nZnO, which were released from the nZnO.[37,38] The ROS, as well as Zn ions, attack the negatively charged bacterial cell wall and cause cell wall leakage, resulting in the death of bacteria.[23] CZBs showed higher activity toward *E. coli*, compared to *S. aureus*, which can be attributed to the presence of a thick layer of peptido glycans in the cell wall of *S. aureus*, compared to *E. coli*.[36,37]

Cell Viability Study. Cell viability data (Figure 7A) showed that both positive control and chitosan control did not show any toxicity at 24, 48, and 72 h in contact with the nHDF cells. CZBs having 0.01% and 0.005% nZnO showed 30%−60% viability after 24 h of incubation. Cell viability of CZBs was increased up to 90% after 48 and 72 h of incubation. All other CZBs (0.0025% and 0.001% nZnO) showed viability in the range of 60%−80% after 24 h of incubation and showed an increase in the viability after 48 and 72 h of incubation. The reduced viability at 24 h was due to the interaction of nZnO with the cells. After 24 h, the remaining viable cells began to multiply and, hence, the viability increased.

Evaluation of Cell Attachment and Infiltration. Cell attachment studies via SEM images (Figures 7B−F) revealed that nHDF cells were attached onto the CZB bandages as well as chitosan control bandages and began to spread on the bandages after 24 h of incubation. This result indicated the cytocompatible nature of the CZBs. This result was further confirmed by the DAPI-stained images of the bandages (Figures 7G−K). The images showed that more cells were attached on CZBs containing a lower concentration of nZnO, in comparison to those with a higher concentration. The cell infiltration images revealed that the nHDF cells penetrated into the interior of the CZBs up to 100 μm after 24 h of incubation (Figure 8). The green color was due to the auto fluorescence of the bandage material, and the red color was due to the actin filaments stained with Phalloidin dye. More cells were attached and filtered on CZBs containing a lower concentration of nZnO, in comparison to those with a higher concentration. The porous nature of the control and composite bandages not only helped the cells to penetrate into the interior but also enhanced the transfer of oxygen and nutrients to cells. The cells that filtered into the interior of the bandages would be helpful for the vascularization, which is very essential in wound healing.[40]

Evaluation of In Vivo Wound Healing and Antibacterial Activity. In vivo study conducted in Sprague−Dawley (SD) rats proved the enhanced wound healing ability of the prepared CZBs. Figure 9 shows photographs of an in vivo wound healing study. Chitosan control as well as CZBs showed excellent healing after one and two weeks, compared to Kaltostat and bare wound. The extent of wound closure was evaluated macroscopically. After two weeks, the wounds treated with the chitosan control and CZBs achieved significant closure to ∼90%, compared to the Kaltostat-treated wound and bare wounds, which showed ∼70% wound closure (Figure 10A). However, complete re-epithelialization was apparent at light microscopy in the sections studied. Furthermore, qualitative histomorphology in routinely stained hematoxilin and eosin sections indicated densely packed keratinocytes in the epidermis on the wounds treated with chitosan control and CZBs, compared to the Kaltostat or bare wound (Figure 11). Furthermore, the presence of nZnO also enhanced the rate of healing in wounds treated with CZBs, which was evident from the H&E-stained images. The extent of collagen deposition was

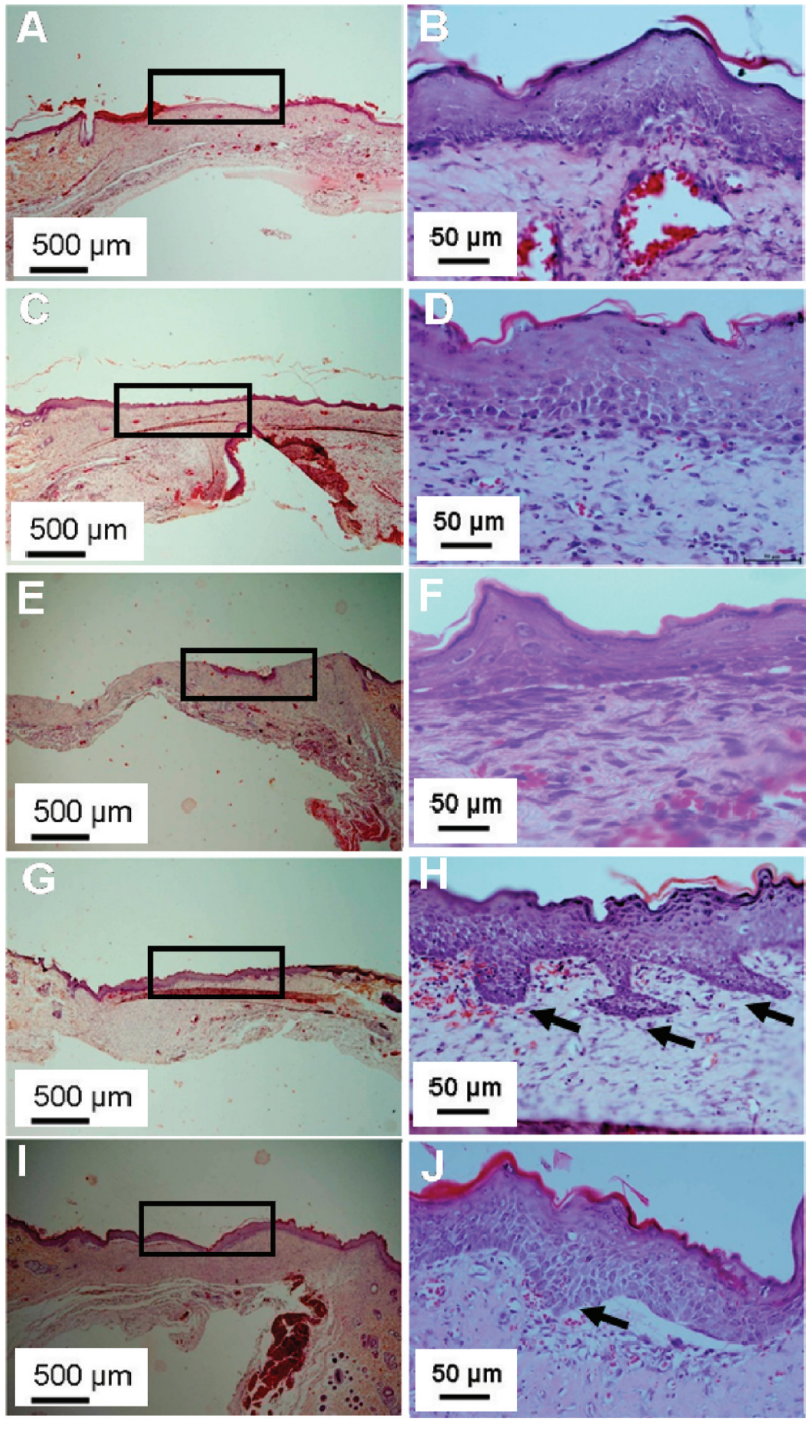

Figure 11. Photomicrographs of hematoxilin and eosin (H&E)-stained (A and B) bare wound, (C and D) Kaltostat-treated wounds, (E and F) chitosan-control-treated wounds, (G and H) chitosan + 0.005% nZnO bandage-treated wounds, and (I and J) chitosan + 0.01% nZnO bandage-treated wounds. Panels A, C, E, G, and I are low-magnification images and panels B, D, F, H, and J are high-magnification images.

estimated by histomorphometry on sections stained with Picro-Sirius Red (Figure 12). By four weeks of healing, there was enhanced collagen deposition in the wound healing assisted by the chitosan controls and the CZBs, compared to the Kaltostat and the bare wounds (Figure 10B). The white colored empty spaces in the images showed the lack of collagen in the bare wound and Kaltostat-treated wounds. There was complete re-epithelialization, as shown in low-magnification photomicrographs (Figure 11). Remarkably there was prominent rete-pegs formation in the wound treated with CZBs, which indicated advanced healing of the neo-epidermis (see black arrows in Figures 11 H and 11J).

Swabs collected from the rat wound were cultured in LB broth for identification as well as quantification. For identification of strains, the inoculums were streaked on a LB agar plate (Figure 13). From the physical appearance, it was determined that there were three types of bacteria and the identification of them was done using various biochemical assays (see Table 1). According to the results obtained via biochemical assays, these bacteria were proven to be

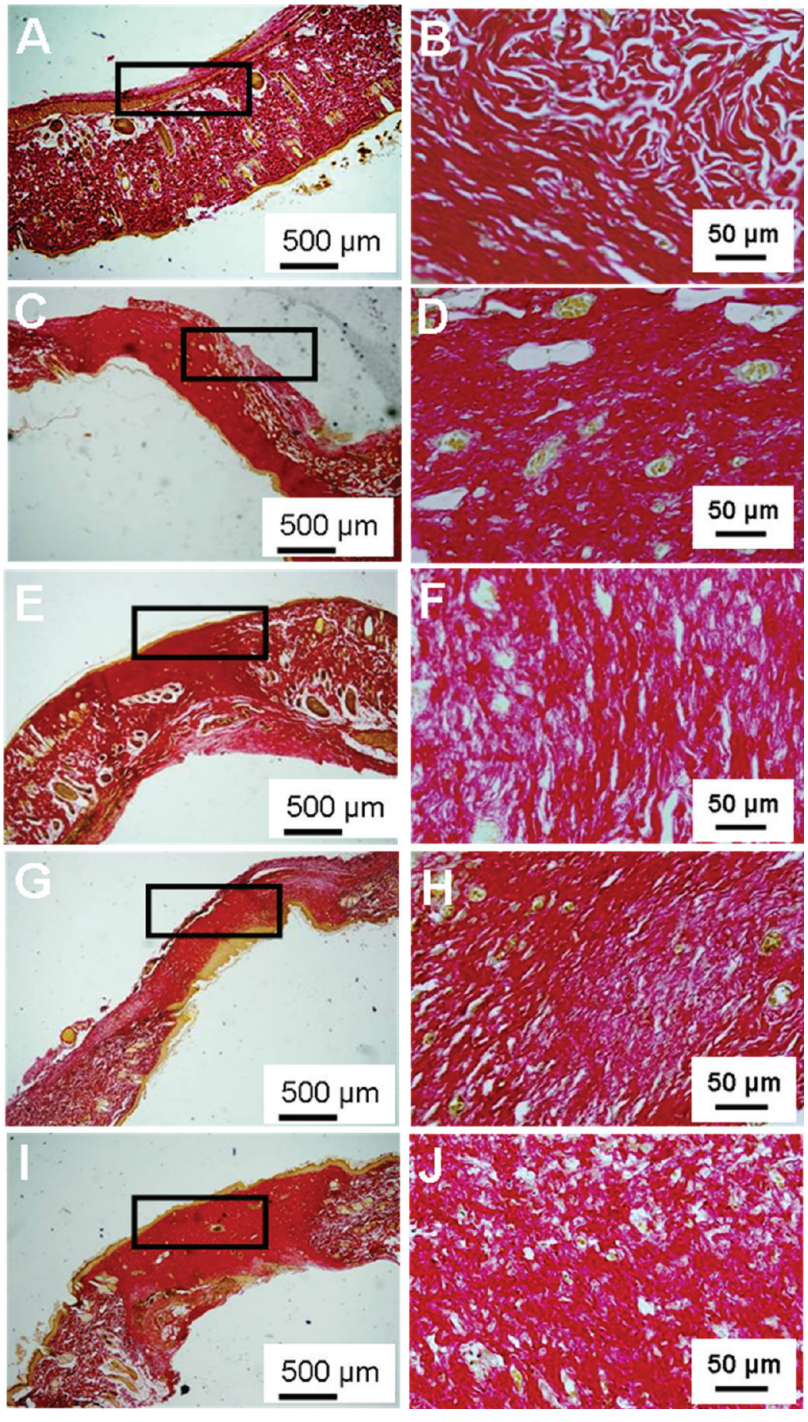

Figure 12. Photomicrographs of Picro-Sirius Red-stained histology sections: (A and B) bare wound, (C and D) Kaltostat-treated wounds, (E and F) chitosan-control-treated wounds, (G and H) chitosan + 0.005% nZnO bandage-treated wounds, and (I and J) chitosan + 0.01% nZnO bandage-treated wounds. Panels A, C, E, G, and I are low-magnification images and panels B, D, F, H, and J are high-magnification images.

Pseudomonas aeruginosa, *Staphylococcus intermedius*, and *Staphylococcus hyicus*. The table clearly indicates that all these bacteria showed reduced viability on wounds treated with CZBs, compared to the chitosan control, Kaltostat, and bare wound (Table 2). The number of viable bacteria was further reduced at Week 2 compared to Week 1 in CZB-treated wounds.

4. CONCLUDING REMARKS

The prepared chitosan hydrogel/nZnO bandages (CZBs) that have interconnected pores showed ~80% porosity of the total bandage volume and were helpful with regard to absorbing large volumes of wound exudate. CZBs showed controlled degradation, enhanced blood clotting, and excellent platelet activation ability. In vitro cytocompatibility studies revealed that the bandages showed enhanced cell viability and infiltration. In vivo wound healing evaluation proved the enhanced healing ability of CZBs without causing toxicity to cells. In vitro and in vivo antibacterial activity studies proved that the antibacterial potential of the prepared CZBs. All these

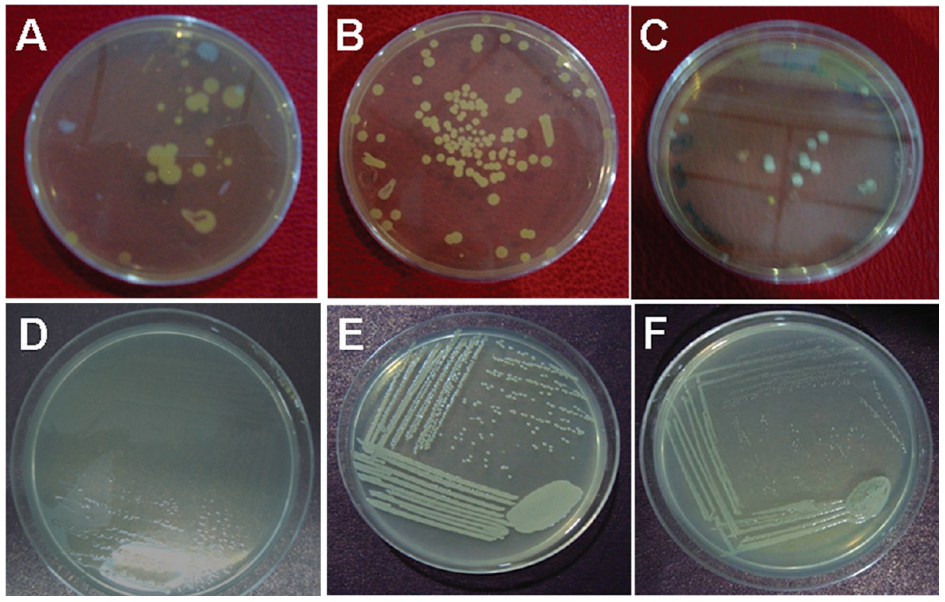

Figure 13. Bacteria isolated from the rat wound after treatment and cultured in LB agar plates: (A, D) *Pseudomonas aeruginosa*, (B, E) *Staphylococcus intermedius*, and (C, F) *Staphylococcus hyicus*. Panels A, B, and C represent samples recultured in LB agar plates, and panels D, E, and F represent samples streaked in LB agar plates.

Table 1. Identification of Bacterial Strain by Biochemical Assays

	Pseudomonas aeruginosa	*Staphylococcus intermedius*	*Staphylococcus hyicus*
gram staining	−	+	+
motility	+	−	−
Voges−Proskauer	−	−	−
green pigment	+	−	−
oxidase	+	−	−
nitrate reduction	+	+	+
citrate (Simmon's)	+	−	−
citrate (Christinsen's)	−	−	−
urease	−	+	+
coagulase	−	+	+
glucose	+	+	−
lactose	−	+	+
maltose	−	+	−
mannitol	+	+	−
salicin	−	−	−
sucrose	−	−	−
xylose	+	−	−
trehalose	−	+	+
fructose	+	+	+

studies indicated that these advanced CZBs can be used for burn, chronic, and diabetic wound infections.

AUTHOR INFORMATION

Corresponding Author

*Tel.: +91-484 2851234. Fax: +91-484 2802020. E-mails: rjayakumar@aims.amrita.edu, jayakumar77@yahoo.com.

Notes

The authors declare no competing financial interest.

ACKNOWLEDGMENTS

One of the authors (R. Jayakumar) is grateful to the Department of Biotechnology (DBT), India, for providing funding (No. BT/PR13885/MED/32/145/2010, dated 03-01-2011). This work also supported by DST, India under a grant of the Nanoscience and Nanotechnology Initiative program. P. T. Sudheesh Kumar acknowledges the Council of Scientific and Industrial Research (CSIR, India) for the financial support through a Senior Research Fellowship (SRF) (Award No. 9/963 (0011) 2K11- EMR-1). The authors are also thankful to Mr. Sajin P. Ravi and Mr. Sarath for their help in SEM and confocal analysis. The authors are grateful to Dr. A. K. K. Unni, Mr. Sunil, Ms. Chandini, and Mr. Sajith for their help during the in vivo study.

Table 2. Quantification of the Rat Wound Bacteria after 1 and 2 Weeks of Treatment

	Pseudomonas aeruginosa		*Staphylococcus intermedius*		*Staphylococcus hyicus*	
wound type	Week 1	Week 2	Week 1	Week 2	Week 1	Week 2
bare wound	2×10^9	2×10^8	3×10^{10}	2×10^8	4×10^{10}	2×10^9
Kaltostat	4×10^9	2×10^8	5×10^{10}	2×10^9	6×10^{10}	8×10^9
chitosan control	7×10^9	4×10^8	9×10^{10}	4×10^9	6×10^{10}	3×10^9
chitosan + 0.01% nZnO	5×10^6	2×10^3	8×10^6	2×10^3	4×10^6	3×10^4
chitosan + 0.005% nZnO	8×10^7	2×10^4	4×10^7	3×10^4	8×10^8	3×10^5

REFERENCES

(1) Willi, P.; Chandra, P. S. *Trends Biomater. Artif. Organs* **2004**, *18*, 18−23.
(2) Jayakumar, R.; Prabaharan, M.; Sudheesh, K. P. T.; Nair, S. V.; Tamura, H. *Biotechnol. Adv.* **2011**, *29*, 322−337.
(3) Madhumathi, K.; Sudheesh, K. P. T; Abilash, S.; Sreeja, V.; Tamura, H.; Manzoor, K. *J. Mater. Sci.: Mater. Med.* **2010**, *21*, 807−813.
(4) Wenzel, R. P.; Perl, T. M. *J. Hosp. Inf.* **1995**, *31*, 13−24.
(5) Gordon, L. A. *Clin. Infect. Dis.* **1998**, *26*, 1179−1181.
(6) Muzzarelli, R. A. A. *Carbohydr. Polym.* **2009**, *76*, 167−182.
(7) Aoyagi, S.; Onishi, H.; Machida, Y. *Int. J. Pharm.* **2007**, *330*, 138−145.
(8) Jayakumar, R.; Menon, D.; Manzoor, K.; Nair, S. V.; Tamura, H. *Carbohydr. Polym.* **2010**, *82*, 227−232.
(9) Burkatovskaya, M.; Castano, A. P.; Demidova, R.T. N.; Tegos, G. P.; Hamblin, M. R. *Wound. Rep. Reg.* **2008**, *16*, 425−431.
(10) Ishihara, M.; Nakanishi., K; Ono, K.; Sato, M.; Kikuchi, M.; Saito, Y. *Biomaterials* **2002**, *23*, 833−840.
(11) Jayakumar, R.; Prabaharan, M.; Nair, S. V.; Tamura, H. *Biotechnol. Adv.* **2010**, *28*, 142−150.
(12) Sudheesh, K. P. T; Abhilash, S.; Manzoor, K.; Nair, S. V.; Tamura, H.; Jayakumar, R. *Carbohydr. Polym.* **2010**, *80*, 761−767.
(13) Jiantao, L.; Caihong, L.; Yi, Z.; Jianchan, H.; Li, M. Z. *ACS Appl. Mater. Interfaces* **2012**, *4*, 1050−1057.
(14) Tao, W.; Xiao, K. Z.; Xu, T. X.; Da, Y. W. *Carbohydr. Polym.* **2012**, *88*, 75−83.
(15) Yen, H. L.; Jung, C.; Ming, C. Y.; Chiang, T. C.; Wen, F. L. *Carbohydr. Polym.* **2012**, *88*, 809−819.
(16) Charernsriwilaiwat, N.; Opanasopit, P.; Rojanarata, T.; Ngawhirunpat, T. *Int. J. Pharm.* **2012**, *427*, 379−384.
(17) Li, X.; Nan, K.; Li, L.; Zhang, Z.; Chen, H. *Carbohydr. Polym.* **2012**, *88*, 84−90.
(18) Clasen, C.; Wilhelms, T.; Kulicke, W. M. *Biomacromolecules* **2006**, *7*, 3210−3222.
(19) Zhou, Y.; Yang, D.; Chen, X.; Xu, Q.; Lu, F.; Nie, J. *Biomacromolecules* **2008**, *9*, 349−354.
(20) Yang, X.; Yang, K.; Wu, S.; Chen, X.; Yu, F.; Li, J. C. *Radiat. Phys. Chem.* **2010**, *79*, 606−611.
(21) Zhang, Z.; Yang, D.; Nie, J. *Int. J. Biol. Macromol.* **2008**, *43*, 456−462.
(22) Jang, S. I.; Mok, J. Y.; Jeon, I. H.; Park, K. H.; Nguyen, T. T. T.; Park, J. S.; Hwang, H. M.; Chai, K. Y. *Molecules* **2012**, *17*, 2992−3007.
(23) Pilakasiri, K.; Molee, P.; Sringernyuang, D.; Sangjun, N.; Channasanon, S.; Tanodekaew, S. *J. Mater. Sci. Mater. Med.* **2011**, *22*, 2497−2504.
(24) Takei, T.; Nakahara, H.; Ijima, H.; Kawakami, K. *Acta. Biomater.* **2012**, *8*, 686−693.
(25) Francesko, A.; Tzanov, T. *Adv. Biochem. Eng. Biotechnol.* **2011**, *125*, 1−27.
(26) Tseng, H. J.; Tsou, T. L.; Wang, H. J.; Hsu, S. H. *J. Tissue Eng. Regen. Med.* **2011**, *4*, 76−84.
(27) Ueno, H.; Mori, T.; Fujinaga, T. *Adv. Drug Delivery Rev.* **2001**, *52*, 105−115.
(28) Tchemtchoua, V. T.; Atanasova, G.; Aqil, A.; Fil, P.; Garbacki, N.; Vanhooteghem, O.; Deroanne, C.; Colige, A. *Biomacromolecules* **2011**, *12*, 3194−3204.
(29) Gupta, B.; Saxena, S.; Arora, A.; Alam, M. S. *Indian J. Fibre Text.* **2011**, *36*, 227−280.
(30) Tsao, C. T.; Chang, C. H.; Li, Y. D.; Wu, M. F.; Lin, C. P.; Han, J. L.; Chen, S. H.; Hsieh, K. H. *J. Bioact. Compat. Polym.* **2011**, *26*, 519−536.
(31) Chia, L. K.; Cheng, L. W.; Horng, H. K.; Weng, S. H.; Kuo, C.; Wang, L. L. *Ceram. Int.* **2010**, *36*, 693−698.
(32) Jalal, R.; Goharshadia, E. K.; Abareshia, M.; Moosavic, M.; Yousefid, A. *Mater. Chem. Phys.* **2010**, *121*, 198−201.
(33) Becheri, A.; Durr, M.; Nostro, P. L.; Baglioni, P. *J. Nanopart. Res.* **2008**, *10*, 679−689.
(34) Alessio, B.; Maximilian, D.; Pierandrea, L. N.; Piero, B. *J. Nanopart. Res.* **2008**, *10*, 679−689.
(35) Kwon, Y. J.; Kim, K. H.; Lim, C. S.; Shim, K. B. *J. Ceram. Proc. Res.* **2002**, *3*, 146−149.
(36) Sawai, J. *Microb. Method.* **2003**, *54*, 177−182.
(37) Nair, S. V.; Abhilash, S.; Divya, R. V. V.; Deepthy, M.; Seema, N.; Manzoor, K. *J. Mater. Sci.: Mater. Med.* **2009**, *20*, 235−241.
(38) Abhilash, S.; Parwathy, C.; Deepthy, M.; Sreerekha, R.; Nair, S. V.; Manzoor, K. *Nanoscale* **2011**, *3*, 3657−3669.
(39) Ong, S. Y.; Wu, J.; Moochhala, S. M.; Tan, M. H.; Lu, J. *Biomaterials* **2008**, *29*, 4323−4332.
(40) Sowmya, S.; Jayakumar, R.; Chennazhi, K. P.; Levorson, E. J.; Mikos, A. G.; Nair, S. V. *Adv. Polym. Sci.* **2012**, *246*, 1−10.